WEST

Generate Collection

Search Results - Record(s) 1 through 2 of 2 returned.

☐ 1. Document ID: US 5840489 A

L3: Entry 1 of 2 File: USPT Nov 24, 1998

US-PAT-NO: 5840489
DOCUMENT-IDENTIFIER: US 5840489 A
TITLE: Diagnosis and treatment of supravalvular aortic stenosis and Williams syndrome

Full | Title | Citation | Front | Review | Classification | Date | Reference | Claims | KWIC | Draw Desc | Image

☐ 2. Document ID: US 5650282 A

L3: Entry 2 of 2 File: USPT Jul 22, 1997

US-PAT-NO: 5650282
DOCUMENT-IDENTIFIER: US 5650282 A
TITLE: Diagnosis of Williams syndrome

Full | Title | Citation | Front | Review | Classification | Date | Reference | Claims | KWIC | Draw Desc | Image

Generate Collection

Terms	Documents
l1 near9 l2	2

Display 20 Documents, starting with Document: 2

Display Format: TI Change Format

Search Results -

Terms	Documents
l3 and (mouse or mice)	0

Database: US Patents Full-Text Database; US Pre-Grant Publication Full-Text Database; JPO Abstracts Database; EPO Abstracts Database; Derwent World Patents Index; IBM Technical Disclosure Bulletins

Refine Search: l3 and (mouse or mice) Clear

Search History

Today's Date: 6/29/2001

DB Name	Query	Hit Count	Set Name
USPT	l3 and (mouse or mice)	0	L6
USPT	l3 and l4	0	L5
USPT	transgen$	7973	L4
USPT	l1 near9 l2	2	L3
USPT	elastin	2119	L2
USPT	knockout or (null adj mutation)	3868	L1

6-29-01

=> d his

(FILE 'HOME' ENTERED AT 16:07:24 ON 29 JUN 2001)

FILE 'MEDLINE, CAPLUS, BIOSIS, SCISEARCH' ENTERED AT 16:07:40 ON 29 JUN 2001

L1 21446 S ELASTIN
L2 44865 S KNOCKOUT OR NULL(W)MUTATION
L3 57 S L1 AND L2
L4 48 S L3 AND (MOUSE OR MICE)
L5 28 DUP REM L4 (20 DUPLICATES REMOVED)
L6 27 S L1(S)L2
L7 22 S L6 AND (MOUSE OR MICE)
L8 10 DUP REM L7 (12 DUPLICATES REMOVED)

=> d au ti so ab 1-10 18

L8 ANSWER 1 OF 10 MEDLINE DUPLICATE 1
AU Johnson J L; Jackson C L
TI Atherosclerotic plaque rupture in the apolipoprotein E knockout **mouse**.
SO ATHEROSCLEROSIS, (2001 Feb 1) 154 (2) 399-406.
Journal code: 95X; 0242543. ISSN: 0021-9150.
AB The rupture of an atherosclerotic plaque is the main underlying cause of coronary artery thrombotic occlusion and subsequent myocardial infarction, but research into the causes and treatment of plaque rupture is hampered by the lack of a suitable animal model. Although complex atherosclerotic plaques can be induced in a number of experimental animal systems, in none of these is plaque rupture an established feature. We have surveyed branch points in the carotid arteries and aortas of apolipoprotein E **knockout mice** fed a diet supplemented with 21% lard and 0.15% cholesterol for up to 14 months. Six male and five female **mice** were used. Four of the male **mice** and four of the female **mice** died, after 46+/-3 weeks of feeding (range 37-59 weeks). Lumenal thrombus associated with atherosclerotic plaque rupture was observed in three male and all four female **mice**. In six of these seven **mice**, an atherosclerotic plaque rupture was found where the brachiocephalic artery branches into the right common carotid and right subclavian arteries. The ruptures were characterised by fragmentation and loss of **elastin** in the fibrous caps of relatively small and lipid-rich plaques overlying large complex lesions, with intraplaque haemorrhage. Immunocytochemical analysis revealed loss of smooth muscle cells from ruptured caps. These data suggest that long-term fat-feeding of apolipoprotein E **knockout mice** is a useful and reproducible model of atherosclerotic plaque rupture, and that these ruptures occur predominantly in the brachiocephalic artery.

L8 ANSWER 2 OF 10 MEDLINE
AU Cawston T; Carrere S; Catterall J; Duggleby R; Elliott S; Shingleton B; Rowan A
TI Matrix metalloproteinases and TIMPs: properties and implications for the treatment of chronic obstructive pulmonary disease.
SO NOVARTIS FOUNDATION SYMPOSIUM, (2001) 234 205-18; discussion 218-28.
Ref:

58
Journal code: C3Y; 9807767.
AB The matrix metalloproteinases (MMPs) are a unique family of metalloenzymes that, once activated, can destroy connective tissue. The active enzymes are all inhibited by tissue inhibitors of metalloproteinases (TIMPs). The relative amounts of active MMPs and TIMPs are important in determining whether tissues are broken down in disease. Although elastase is often regarded as the target enzyme in chronic obstructive pulmonary disease (COPD), both the neutrophils and macrophages in the lung contain metalloproteinases and both collagen and **elastin** are degraded in disease. Transgenic studies have shown that when MMP1 is over-expressed, pulmonary emphysema develops in **mice**, while MMP12 **knockout mice** do not develop pulmonary emphysema when exposed to cigarette smoke. New drugs that can specifically block active MMPs are now available. These potent inhibitors are effective in vitro and prevent the destruction of tissue in animal models. Future patient trials will test the effectiveness of these compounds in preventing tissue destruction.

L8 ANSWER 3 OF 10 MEDLINE DUPLICATE 2
AU Shipley J M; Mecham R P; Maus E; Bonadio J; Rosenbloom J; McCarthy R T; Baumann M L; Frankfater C; Segade F; Shapiro S D
TI Developmental expression of latent transforming growth factor beta binding protein 2 and its requirement early in **mouse** development.
SO MOLECULAR AND CELLULAR BIOLOGY, (2000 Jul) 20 (13) 4879-87.
Journal code: NGY; 8109087. ISSN: 0270-7306.
AB Latent transforming growth factor beta (TGF-beta) binding protein 2 (LTBP-2) is an integral component of **elastin**-containing microfibrils. We studied the expression of LTBP-2 in the developing **mouse** and rat by in situ hybridization, using tropoelastin expression as a marker of tissues participating in elastic fiber formation. LTBP-2 colocalized with tropoelastin within the perichondrium, lung, dermis, large arterial vessels, epicardium, pericardium, and heart valves at various stages of rodent embryonic development. Both LTBP-2 and tropoelastin expression were seen throughout the lung parenchyma and within the cortex of the spleen in the young adult **mouse**. In the testes, LTBP-2 expression was seen within lumenal cells of the epididymis in the absence of tropoelastin. Collectively, these results imply that LTBP-2 plays a structural role within elastic fibers in most cases. To investigate its importance in development, **mice** with a targeted disruption of the Ltbp2 gene were generated. Ltbp2(-/-) **mice** die between embryonic day 3.5 (E3.5) and E6.5. LTBP-2 expression was not detected by in situ hybridization in E6.5 embryos but was detected in E3.5 blastocysts by reverse transcription-PCR. These results are not consistent with the phenotypes of TGF-beta **knockout mice** or **mice** with **knockouts** of other elastic fiber proteins, implying that LTBP-2 performs a yet undiscovered function in early development, perhaps in implantation.

L8 ANSWER 4 OF 10 MEDLINE DUPLICATE 3
AU Starcher B
TI Role for tumour necrosis factor-alpha receptors in ultraviolet-induced skin tumours.
SO BRITISH JOURNAL OF DERMATOLOGY, (2000 Jun) 142 (6) 1140-7.

Journal code: AWO; 0004041. ISSN: 0007-0963.

AB The biological effects of tumour necrosis factor (TNF)-alpha are mediated through either the TNFR1 or the TNFR2 receptor. In the present study, the effects of ultraviolet (UV) irradiation on skin pathology and tumour promotion were studied in hairless **mice** deficient in either the TNFR1 or the TNFR2 receptor. SKH-1 hairless **mice** were crossed with either TNFR1 **knockout** (KO) **mice** or TNFR2 KO **mice** to develop a strain of hairless **mice** deficient in either of these receptors. Elastosis and other pathological indications of UVB irradiation were not affected by the loss of either receptor. The absence of either receptor, however, resulted in a highly significant reduction in skin tumours in response to UVB irradiation. Inflammatory cell influx following chronic UV irradiation was virtually eliminated in the TNFR1 KO **mice**, while the TNFR2 KO **mice** responded to UV irradiation with the normal increase in inflammatory cells throughout the lower and upper dermis. Contact hypersensitivity responses were eliminated in the TNFR2 KO **mice**, whereas the TNFR1 KO **mice** retained normal contact hypersensitivity reactions. These studies suggest that TNF-alpha plays no part in the accumulation of excessive **elastin** in the skin during chronic UVB exposure. However, there appears to be an important role for TNF-alpha in mediating tumorigenesis, distinct from its role in initiating cutaneous immune responses.

L8 ANSWER 5 OF 10 MEDLINE DUPLICATE 4

AU Faury G; Maher G M; Li D Y; Keating M T; Mecham R P; Boyle W A

TI Relation between outer and luminal diameter in cannulated arteries.

SO AMERICAN JOURNAL OF PHYSIOLOGY, (1999 Nov) 277 (5 Pt 2) H1745-53. Journal code: 3U8; 0370511. ISSN: 0002-9513.

AB Resistance in blood vessels is directly related to the inner (luminal) diameter (ID). However, ID can be difficult to measure during physiological experiments because of poor transillumination of thick-walled or tightly constricted vessels. We investigated whether the wall cross-sectional area (WCSA) in cannulated arteries is nearly constant, allowing IDs to be calculated from outer diameters (OD) using a single determination of WCSA. With the use of image analysis, OD and ID were directly measured using either transillumination or a fluorescent marker in the lumen. IDs from a variety of vessel types were calculated from WCSA at several reference pressures. Calculated IDs at all of the reference WCSA were within 5% (mean <1%) of the corresponding measured IDs in all vessel types studied, including vessels from heterozygote **elastin knockout** animals. This was true over a wide range of transmural pressures, during treatment with agonists, and before and after treatment with KCN. In conclusion, WCSA remains virtually constant in cannulated vessels, allowing accurate determination of ID from OD measurement under a variety of experimental conditions.

L8 ANSWER 6 OF 10 MEDLINE

AU Warburton D; Lee M K

TI Current concepts on lung development.

SO CURRENT OPINION IN PEDIATRICS, (1999 Jun) 11 (3) 188-92. Ref: 23 Journal code: BUT; 9000850. ISSN: 1040-8703.

AB Recent molecular genetic and embryonic organ culture studies have implicated several novel regulatory processes in the coordination of lung development. Failure of pulmonary initiation results from interruptions of

the sonic hedgehog/patched/Gli and Nl alpha 2.1 signaling pathways. Sonic hedgehog null mutants and Gli2/Gli3 compound null mutants each exhibited failed tracheoesophageal septation. However, proximodistal epithelial differentiation is disrupted by compound Gli mutation, but is preserved in sonic hedgehog mutants. **Null mutation** of Nl alpha 2.1 also abrogates tracheoesophageal septation in association with thyroid and pituitary agenesis. Primary tracheal branching is regulated by fibroblast growth factor-10 signaling; in the murine fibroblast growth factor-10 null phenotype, the lung fails to separate from the foregut and morphogenesis is arrested distal to the trachea. Several genes in the fibroblast growth factor-10 pathway have homologous roles in fruit fly tracheal organogenesis, and corresponding Drosophila mutations yield strikingly similar phenotypes. Recent data also indicate that airway branching can be regulated by vascular endothelial growth factor, suggesting mutual regulation of airway and vascular development. The bases of pulmonary left-right asymmetry and laterality have also been investigated. The transforming growth factor-beta superfamily members Lefty-1, Lefty-2, and nodal comprise a regulatory pathway whose function is required for the development of left-right asymmetry, whereas left-right laterality is dependent on regulation of dynein expression by the transcription factor hepatocyte nuclear factor-4. Terminal lung differentiation is modulated by yet another set of signals. Hoxa5 null mutants exhibit tracheal occlusion and surfactant protein deficiency, whereas fibroblast growth factor receptor-2 and -4 compound null phenotypes include abrogated neonatal alveolization, perturbed alveolar myofibroblast differentiation, and persistent neonatal **elastin** deposition. These new contributions represent substantial advances toward a comprehensive molecular model of pulmonary development.

L8 ANSWER 7 OF 10 MEDLINE DUPLICATE 5
AU Koglin J; Glysing-Jensen T; Raisanen-Sokolowski A; Russell M E
TI Immune sources of transforming growth factor-beta1 reduce transplant arteriosclerosis: insight derived from a knockout **mouse** model.
SO CIRCULATION RESEARCH, (1998 Sep 21) 83 (6) 652-60.
Journal code: DAJ; 0047103. ISSN: 0009-7330.
AB Activated CD4-positive T cells are essential in the early stages of arteriosclerotic lesion development after cardiac transplantation. Besides its parenchymal effects, transforming growth factor-beta1 (TGF-beta1) mediates immunosuppressive effects on proliferation and activation of CD4 cells. This study was designed to assess immune contributions of TGF-beta1 to arteriosclerosis by comparing the effect of TGF-beta1-deficient and -competent infiltrating inflammatory cells on the development of intimal thickening in a heterotopic **mouse** transplant model (CBA to C57B6). Transplant arteriosclerosis was evaluated in cardiac grafts placed into **knockout** recipients heterozygous for TGF-beta1 (n=7) and was compared with those placed into wild-type recipients (n=11). At 55 days, allografts in TGF-beta1-deficient recipients had increased concentric intimal thickening. Computer-assisted analysis of all **elastin**-positive vessels (n=173) showed significantly increased luminal occlusion (67.8+/-5.6%) in grafts from TGF-beta1-deficient recipients compared with wild-type recipients (47.4+/-4.1%, P=0.003). To

determine whether TGF-beta1 deficiency altered CD4 activation patterns, we studied intragraft cytokine expression. Using 32P-reverse-transcriptase polymerase chain reaction assays, we show that TGF-beta1-deficient recipients had an increased expression of the transcription factor STAT 4, interferon gamma, and interleukin-2 (Th1-type response) and unaltered or reduced expression of the transcription factor STAT 6, interleukin-4, and interleukin-10 (Th2-type response). Hence, when present, immune sources of TGF-beta1 attenuate transplant arteriosclerosis. This effect is associated with attenuation of Th1 forces.

L8 ANSWER 8 OF 10 MEDLINE DUPLICATE 6
AU Mottram P L; Raisanen-Sokolowski A; Glysing-Jensen T; Stein-Oakley A N; Russell M E
TI Cardiac allografts from IL-4 knockout recipients: assessment of transplant arteriosclerosis and peripheral tolerance.
SO JOURNAL OF IMMUNOLOGY, (1998 Jul 15) 161 (2) 602-9.
Journal code: IFB; 2985117R. ISSN: 0022-1767.
AB To study the role of IL-4 in tolerance induction and transplant arteriosclerosis, BALB/c hearts were transplanted into C57BL/6J wild-type or IL-4 **knockout** (IL-4(-/-)) recipients. A 30-day course of anti-CD4/8 mAb was used to induce long term graft survival. Primary graft survival was 50% (5 of 10) in IL-4(-/-) recipients comparable to 63% (5 of 8) in wild-type recipients. **Mice** with allografts surviving >80 days were tested for tolerance by challenge with a second donor or third party (CBA) heart. Secondary donor-strain heart grafts survived >30 days, but showed histologic evidence of ongoing alloimmune response. Third party hearts rejected rapidly. Although immunostaining and 32P RT-PCR assays showed no differences in the mononuclear cell infiltration and T cell activation between IL-4(-/-) and wild-type tolerant recipients, some monokines (IL-12, TNF-alpha, and allograft inflammatory factor-1) were up-regulated in grafts from IL-4(-/-) recipients. Computer-assisted analysis of **elastin**-stained vessels revealed that the severity of vascular thickening (percentage of luminal occlusion, mean +/- SD, n = 329) was similar in grafts from IL-4(-/-) (63.7 +/- 16.9%) and wild-type (69.5 +/- 17.6%) recipients. Thus, IL-4 deficiency did not alter primary or secondary graft survival, infiltration, or vascular thickening. The selective alterations in monokine expression suggests that alternative pathways are activated and may compensate in IL-4(-/-) **mice**.

L8 ANSWER 9 OF 10 MEDLINE DUPLICATE 7
AU Morris C A
TI Genetic aspects of supravalvular aortic stenosis.
SO CURRENT OPINION IN CARDIOLOGY, (1998 May) 13 (3) 214-9. Ref: 56
Journal code: BDA; 8608087. ISSN: 0268-4705.
AB Supravalvular aortic stenosis (SVAS) occurs as an autosomal dominant trait or as part of the phenotype of the usually sporadic condition Williams syndrome. SVAS is the result of mutation or deletion of the **elastin** gene (ELN), located at chromosome 7q11.23. Thus, SVAS may be more appropriately termed an **elastin** arteriopathy. Studies have demonstrated various point mutations and intragenic deletions of ELN resulting in nonsyndromic SVAS. Individuals with Williams syndrome are

hemizygous for the **elastin** gene, owing to a 1 to 2 megabase deletion of a portion of the long arm of chromosome 7 that encompasses ELN. This submicroscopic deletion is readily detected by fluorescent in-situ hybridization, useful in the diagnosis of Williams syndrome. The severity of SVAS is quite variable, both in series of Williams syndrome patients and within SVAS kindreds, suggesting that other genetic factors are involved in expression of the phenotype. Experiments with **elastin knockout mice** will likely yield clues regarding the role of **elastin** in arterial morphogenesis and the pathogenesis of obstructive vascular disease.

L8 ANSWER 10 OF 10 MEDLINE DUPLICATE 8
AU Burn J; Goodship J
TI Developmental genetics of the heart.
SO CURRENT OPINION IN GENETICS AND DEVELOPMENT, (1996 Jun) 6 (3) 322-5.
Ref: 34
Journal code: BJC; 9111375. ISSN: 0959-437X.
AB Studies of children with heart defects and chromosomal anomalies have led to the discovery that loss of an **elastin** gene can cause supravalvar aortic stenosis and that a 2 Mb deletion from 22q11 is second only to Down's syndrome as a cause of heart defects. Molecular dissection of the 22q11 region to find the genes which produce the outflow-tract defects and other disorders of neural crest migration has proven more difficult, as there are a large number of genes in the deleted region. Classic mapping studies have located a gene which can cause total anomalous venous drainage near the centromere of chromosome 4. **Knockout mouse** studies have demonstrated an important role in cardiac development for, amongst others, endothelin-1 and neuregulin. Functional redundancy and maternal rescue are two reasons why **knockouts** do not always live up to our expectations. Serendipitous findings in the **mouse** are equally important. Work continues to isolate the inversion of embryo turning (inv) gene which invariably disturb the left-->right gradient in homozygotes, causing heart defects in many instances. Sadly, the original insertional mutation has resulted in a complex deletion duplication which has slowed discovery of the coding sequence.

=>

STIC-ILL

From: Chen, Shin-Lin
Sent: Friday, June 29, 2001 4:26 PM
To: STIC-ILL
Subject: article

please provide the following articles ASAP. Thanks!
Serial No. 09/258,217.

L8 ANSWER 5 OF 10 MEDLINE DUPLICATE 4
AU Faury G; Maher G M; Li D Y; Keating M T; Mecham R P; Boyle W A
TI Relation between outer and luminal diameter in cannulated arteries.
SO AMERICAN JOURNAL OF PHYSIOLOGY, (1999 Nov) 277 (5 Pt 2) H1745-53.
Journal code: 3U8; 0370511. ISSN: 0002-9513.

L8 ANSWER 9 OF 10 MEDLINE DUPLICATE 7
AU Morris C A
TI Genetic aspects of supravalvular aortic stenosis.
SO CURRENT OPINION IN CARDIOLOGY, (1998 May) 13 (3) 214-9. Ref: 56
Journal code: BDA; 8608087. ISSN: 0268-4705.
(Please provide this reference first)

L8 ANSWER 10 OF 10 MEDLINE DUPLICATE 8
AU Burn J; Goodship J
TI Developmental genetics of the heart.
SO CURRENT OPINION IN GENETICS AND DEVELOPMENT, (1996 Jun) 6 (3) 322-5. Ref: 34.

Shin-Lin Chen
AU 1633
CM1 12A15
(703)305-1678

Article title	Developmental genetics of the heart
Article identifier	0959437X96000546
Authors	Burn_J Goodship_J
Journal title	Current Opinion in Genetics and Development
ISSN	0959-437X
Publisher	Current Biology
Year of publication	1996
Volume	6
Issue	3
Supplement	0
Page range	322-325
Number of pages	4
User name	Adonis
Cost centre	Development
PCC	$12.00
Date and time	Friday, June 29, 2001 5:42:36 PM

Developmental genetics of the heart

John Burn* and Judith Goodship†

Studies of children with heart defects and chromosomal anomalies have led to the discovery that loss of an elastin gene can cause supravalvar aortic stenosis and that a 2 Mb deletion from 22q11 is second only to Down's syndrome as a cause of heart defects. Molecular dissection of the 22q11 region to find the genes which produce the outflow-tract defects and other disorders of neural crest migration has proven more difficult, as there are a large number of genes in the deleted region. Classic mapping studies have located a gene which can cause total anomalous venous drainage near the centromere of chromosome 4. Knockout mouse studies have demonstrated an important role in cardiac development for, amongst others, endothelin-1 and neuregulin. Functional redundancy and maternal rescue are two reasons why knockouts do not always live up to our expectations. Serendipitous findings in the mouse are equally important. Work continues to isolate the *inversion of embryo turning* (*inv*) gene which invariably disturbs the left→right gradient in homozygotes, causing heart defects in many instances. Sadly, the original insertional mutation has resulted in a complex deletion duplication which has slowed discovery of the coding sequence.

Address
Department of Human Genetics, University of Newcastle upon Tyne, 19/20 Claremont Place, Newcastle upon Tyne NE2 4AA, UK
*e-mail: john burn@ncl.ac.uk
†e-mail: j a goodship@ncl.ac.uk

Current Opinion in Genetics & Development 1996, 6:322–326

Abbreviations

CATCH22	cardiac defects, abnormal facies, thymic hypoplasia, cleft palate and hypocalcaemia resulting from 22q11 deletions
DGCR	DiGeorge syndrome critical region
inv	*inversion of embryo turning*

Introduction

Where to begin? This question has deterred many from even thinking of studying the genetic basis of human heart development and maldevelopment. The existence of major developmental genes liable to display Mendelian properties when defective was considered improbable until recently. As the importance of single gene defects became more obvious, the complexity of converting a tube of mesodermal cells into a complex four-chamber pump, while it is in constant use, provided a further deterrent to all but the farsighted or foolhardy. Now, at last, the power of both molecular genetics and experimental embryology have reached a point at which the genetic understanding of cardiac development is within reach.

Cytogenetic clues

From our clinical perspective, malformation is a driving force, both as a reason for study and as a source of experimental approach. The study of chromosome aneuploidy provided the first genetic advance in the demonstration that trisomy 21 causes 5% of heart defects in general and most cases of isolated atrioventricular septal defects. The major advance in recent months has resulted from a balanced 6;7 chromosome translocation associated with the supravalvar aortic stenosis, the characteristic heart defect of William's syndrome [1]. Demonstration of deletion of the elastin gene in syndromic cases and disruption of the gene in children with the isolated abnormality of the aorta [2] has provided a major insight into both the clinical disorder and the cellular mechanisms involved in aortic development. Olson *et al.* [3] have recently found that a 30 kb deletion within the elastin gene is associated with a severe form of supravalvar aortic stenosis and peripheral pulmonary artery stenoses. This demonstrates that loss of one allele of the elastin gene is sufficient to produce the cardiovascular phenotype.

Another genetic cause of heart malformation of an even greater significance, where the molecular genetics has not proved to be as simple as the elastin gene deletion, is the 22q11 deletion. The recognition that submicroscopic deletions of chromosome 22q11 are responsible for the vast majority of cases of DiGeorge syndrome and a spectrum of overlapping phenotypes that can be summarised by the acronym CATCH22 (cardiac defects, abnormal facies, thymic hypoplasia, cleft palate and hypocalcaemia resulting from 22q11 deletions) [4] had led us to assume that, in a short time, we would have identified a gene with a key role in cardiac development. The heart defects most commonly seen in CATCH22 are interrupted aortic arch, truncus arteriosus, pulmonary atresia/ventricular septal defect and preliminary studies suggest that 30–50% of cases of interrupted aortic arch and truncus arteriosus are secondary to this chromosomal deletion. However, things have turned out to be far more complex than expected and—despite intensive work by a number of groups over the past 5 years—the gene or genes responsible for the cardiac phenotype have not been identified (or if they have been identified they have not been proven to be such). In the majority of children with deletions, 2 Mb of DNA is removed; the map illustrated as Figure 1 details the genes which have been cloned in this region [5–15]. The DiGeorge syndrome critical region (DGCR), delineated from smaller deletions and which includes the only balanced translocation breakpoint, known as ADU [16], reported in DiGeorge syndrome, has also

been defined and most groups have concentrated on the isolation and investigation of genes in this region.

The transcription factor TUPLE1 (also known as DGCR-1) remains a strong contender for a pivotal role in the failure of neural crest migration [5]. Although it is not disrupted by the translocation, *TUPLE1* is clearly expressed in the face, branchial arches and outflow tract of the heart. Philipe and co-workers [17•] have reported a child who has truncus arteriosus, a typical dysmorphic facial appearance and a deletion which is telomeric to the balanced translocation breakpoint but includes *TUPLE1*. Scambler and co-workers [18•] have recently identified a transcribed, spliced, polyadenylated gene with no apparent protein product (nominated name *DGCR-5*) which has exons on either side of the balanced translocation breakpoint, raising the possibility that this gene may be a controlling element required for transcription of one or more downstream genes. At present, it is still not clear whether the CATCH22 phenotype results from deletion of a single gene or a combination of genes.

Positional cloning

The traditional approach of linkage mapping has yielded relatively few cardiac development genes because of the difficulty of collecting families with a sufficient number of living affected members. A recent important exception has been the mapping of a gene for total anomalous venous drainage to the centromeric region of chromosome 4 [19]. By using samples from a large Idaho family, Bleyl *et al.* [19] achieved a maximum lod score of 6.51 at θ 0.00. Only seven affected individuals were available for study. With at least one obligate carrier showing no evidence of abnormality and the possibility that asypmtomatic relatives had only partial anomalous drainage, the analysis treated all but the seven affected and linking obligate carriers as being of unknown phenotype. The success of the mapping exercise with this restriction demonstrates the power of this approach given the density of markers now available.

Transgenic knockout mice

An alternative approach to reliance on spontaneous human models is the deliberate generation of transgenic mice with a loss of function mutation in a gene of potential importance. This approach has produced valuable information in several experiments. Kurihara *et al.* [20] created a knockout for the endothelin-1 gene, the product of which was first identified as a vasoconstrictor and was postulated to have a role in cardiovascular homeostasis and a pathological role in hypertension. Heart development was impaired with outflow tract anomalies, including aortic arch defects and ventricular septal defects. The similarity to defects associated with neural crest ablation prompted speculation that endothelin-1 has a role in neural crest migration. Other important developmental genes studied in this way have been *neuregulin*, *erbB2* and *erbB4* [21–23]. Neuregulin is a member of the epidermal growth factor family, and erbB2 and erbB4 are two of its receptors. Neuregulin knockouts die *in utero* and have a deficit of ventricular trabeculae and a deficiency of mesenchymal cells in the endocardial cushions. ErbB2 and erbB4 knockouts also lack trabeculae, but the effects on the endothelial cushions are not as pronounced. Neuregulin is expressed in the endothelium and its receptors are expressed in the myocardium, suggesting that neuregulin has a paracrine effect on myocardial development through its receptors.

Expression studies have been interpreted to suggest that transforming growth factor β1 is of critical importance in heart development, yet no heart malformation has been found in transforming growth factor β1 knockout mice; death results instead from multifocal inflammatory disorders at the postnatal stage [24]. Protein levels in the mice were found to be normal, prompting the

Figure 1

This figure shows the position of the genes that have been cloned in the commonly deleted region relative to the balanced translocation breakpoint ADU. The shaded regions represent the DiGeorge critical region (DGCR), with its distal margin delineated by a cell line GM0980 from an affected individual with the unbalanced products of an 11;22 translocation leading to monosomy 22pter–q11, the commonly deleted region, and patient G, who has truncus arteriosus and dysmorphic facial appearance [17•]. DGCR-1 [5,6], DGCR-2 [9,10,13], DGCR-3 and DGCR-4 [13], DGCR-5 (nominated name not yet approved by the nomenclature committee) [18•], COMT1 [34], T10 [7], ZNZF4 [8], LZTR-1 [11].

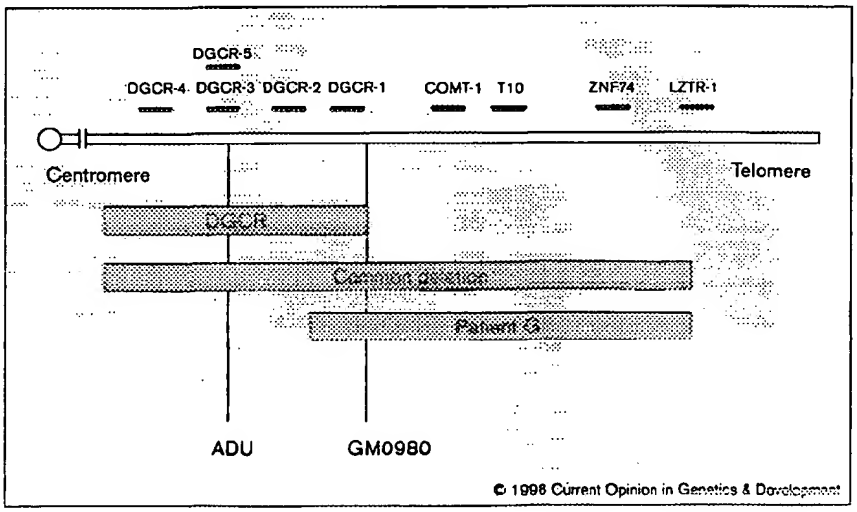

theory that maternal rescue accounts for survival; this was subsequently shown to be the case [25]. Suppression of the immune response in null females to procure 'unrescued' mice has revealed severe cardiac malformations. This work gives substance to a theory put forward several years ago that the familial pattern of neural tube defects could be interpreted as being dependent on the maternal and fetal genotype acting as a combined unit (in effect, four alleles instead of two). The observation that heart defects are more common in the offspring of affected mothers than of unaffected mothers has been interpreted as being a possible consequence of imprinting. Again, the possibility of failure of maternal rescue when the gene defect is inherited from the mother provides an interesting alternative perspective.

The polygenic model for malformations remains of relevance as illustrated by the report of Threadgill *et al.* [26], who examined mice with a knockout of the epidermal growth factor receptor. On one genetic background the embryos died preimplantation, in another they died during embryogenesis, and in a third the mice lived for up to three weeks after birth. These mice did not have heart defects, but the message is clearly of relevance to all knockout experiments. The gene for tenascin displays a highly restricted expression pattern in the heart, yet knockout mice — even those born to 'knockout mothers' — had no heart defect [27]. It seems likely that manipulation of candidate genes in mouse models will grow in strength as a research tool but it is unlikely to diminish the need for the other approaches.

Mouse serendipity

Just as some knockout mice don't have heart defects when they were expected to, others studied for different reasons yield important information. From the cardiac perspective, the most important knockout experiment resulted from the attempts of Yokoyama *et al.* [28] to investigate molecular approaches to the tyrosinase gene, defects in which underlie oculocutaneous albinism; the insertional mutant *inversion of embryo turning* (*inv*) being the result. In contrast to the long established iv/iv mutant, in which the direction of laterality is random, the new model displayed partial or complete *situs inversus* in all homozygotes. In addition to renal and liver pathology, *inv* homozygotes have complex heart defects similar to those seen in humans with isomerism sequence. Identification of the coding sequence has been slowed by the fact the the original insertional knockout has produced a complex duplication/deletion [29]. The heart is uniquely sensitive to any disturbance of laterality because its development as an asymmetric midline organ depends on a clear determination of the left→right gradient. Understanding the genetic control of formation of the left→right gradient will be an important step towards understanding heart formation.

Murine/human correlation

An assumption that underlies studies of such mouse mutants is that we will be able to transfer knowledge to the study of humans with heart defects. One case where this approach may have led to confusion has been with the study of connexin 43. Following reports of obstruction to the right ventricular outflow tract in mice with a connexin 43 knockout [30°], Britz-Cunningham *et al.* [31°] found that of the six human hearts with visceroatrial heterotaxia in a series of 30 pathology specimens all had mutations near the carboxyl terminus of connexin 43, and that four had two mutations suggestive of a recessive defect. Attempts to replicate this work, however, have been unsuccessful; the analysis of 40 comparable cases in our centre and elsewhere has failed to demonstrate a single *connexin 43* mutation [32,33]. Despite this particular example, there can be little doubt that the isolation of genes involved in the development of the heart in the mouse — as is being attempted by several groups — with subsequent human analysis, is a logical way forward.

Conclusions

The convergence of positional cloning studies in man — aided by the study of children with chromosomal deletions and the discoveries resulting from the intentional and serendipitous disruption of cardiac genes in the mouse — has led to a rapid advance in our understanding of the genetic control of heart formation. Given the complexity of the process, however, it is likely that it will be several years before we understand fully what makes us tick.

References and recommended reading

Papers of particular interest, published within the annual period of review, have been highlighted as:

- ° of special interest
- °° of outstanding interest

1. Curran ME, Atkinson DL, Ewart AK, Morris CA, Leppert MF, Keating MT: **The elastin gene is disrupted by a translocation associated with supravalvular aortic stenosis.** *Cell* 1993, 73:159–168.

2. Ewart AK, Jin W, Atkinson D, Morris CA, Keating MT: **Supravalvular aortic stenosis associated with a deletion disrupting the elastin gene.** *J Clin Invest* 1994, 93:1071–1077.

3. Olson TM, Michels VV, Urban Z, Csisztar K, Christiano AM, Driscoll DJ, Feldt RH, Boyd CD, Thibodeau SN: **A 30 kb deletion within the elastin gene results in familial supravalvular aortic stenosis.** *Hum Mol Genet* 1995, 4:1677–1679.

4. Wilson DI, Burn J, Scambler P, Goodship J: **Di George syndrome: part of CATCH 22.** *J Med Genet* 1993, 30:852–856.

5. Halford S, Wadey R, Roberts C, Daw SCM, Whiting JA, O'Donnell H, Dunham I, Bentley D, Lindsay E, Baldini A *et al.*: **Isolation of a putative transcriptional regulator from the region of 22q11 deleted in DI George syndrome, Shprintzen syndrome and familial congenital heart disease.** *Hum Mol Genet* 1993, 2:2099–2107.

6. Lamour V, Lécluse Y, Desmaze C, Spector M, Bodescot M, Aurias A, Osley MA, Lipinski M: **A human homolog of the *S. cerevisiae HIR1* and *HIR2* transcriptional repressors cloned from the DiGeorge syndrome critical region.** *Hum Mol Genet* 1995, 4:791–799.

7. Halford S, Wilson DJ, Daw SCM, Roberts C, Wadey R, Kamath S, Wickremansinghe A, Burn J, Goodship J, Mattei M-G *et al.*: **Isolation of a gene expressed during early embryogenesis from the region of 22q11 commonly deleted in DiGeorge syndrome.** *Hum Mol Genet* 1993, 2:1577–1582.

8. Aubry M, Demczuk S, Desmaze C, Aikem M, Aurias A, Julien J, Rouleau GA: **Isolation of a zinc finger gene consistently deleted in DiGeorge syndrome.** *Hum Mol Genet* 1993, 2:1583–1587.

9. Demczuk S, Aledo R, Zucman J, Delattre O, Desmaze C, Dauphinot L, Jalbert P, Rousleau GA, Thomas G, Aurias A: **Cloning of a balanced translocation breakpoint in the DiGeorge syndrome critical region and isolation of a novel potential adhesion receptor gene in its vicinity.** *Hum Mol Genet* 1995, 4:551–558.

10. Wadey R, Daw S, Taylor C, Atif U, Kamath S, Halford S O'Donnell H, Wilson D, Goodship J, Burn J, Scambler P: **Isolation of a gene encoding an integral membrane protein from the vicinity of a balanced breakpoint associated with DiGeorge syndrome.** *Hum Mol Genet* 1995, 4:1027–1033.

11. Kurahashi H, Akagi K, Inazawa J, Ohta T, Niikawa N, Kayatani F, Sano T, Okada S, Nishito J: **Isolation and characterization of a novel gene deleted in DiGeorge syndrome.** *Hum Mol Genet* 1995, 4:541–549.

12. Budarf ML, Konkle BA, Ludlow LB, Michaud D, Li M, Yamashiro DJ, McDonald-McGinn D, Zackai EH, Driscoll DA: **Identification of a patient with Bernard–Soulier syndrome and a deletion in the DiGeorge/Velo-cardio-facial chromosomal region in 22q11.2.** *Hum Mol Genet* 1995; 4:763–766.

13. Budarf ML, Collins J, Gong W, Roe B, Wang Z, Bailey LC, Sellinger B, Michaud D, Driscoll DA, Emanuel BS: **Cloning a balanced translocation associated with DiGeorge syndrome and identification of a disrupted candidate gene.** *Nat Genet* 1995, 10:269–278.

14. Kelly MD, Essex DW, Shapiro SS, Meloni J, Druck T, Huebner K, Konkle BA: **Complementary DNA cloning of the alternatively expressed endothelial cell glycoprotein Ibb (GPIbb) and localization of the *GPIbb* gene to chromosome 22.** *J Clin Invest* 1994, 93:2417–2424.

15. Pizzuti A, Novelli G, Mari A, Ratti A, Colosimo A, Amati F, Penso D, Sanguiolo F, Calabrese G, Palka G: **Human homologue sequences to the *Drosophila dishevelled* segment-polarity gene are deleted in the DiGeorge syndrome.** *Am J Hum Genet* 1996, 58:722–729.

16. Augusseau S, Jouk PS, Jalbert P, Prieur M: **DiGeorge syndrome and 22q11 rearrangements.** *Hum Genet* 1986, 74:206.

17. ° Levy A, Demczuk S, Aurias A, Depétris D, Mattei M, Philipe N: **Interstitial 22q11 microdeletion excluding the ADU breakpoint in a patient with DiGeorge syndrome.** *Hum Mol Genet* 1995, 4:2417–2419.

Much effort in the search for the gene, or genes, responsible for the CATCH22 phenotype has been directed towards cloning the breakpoint in a patient with a balanced translocation, and this had been achieved by three groups independently. This report describes a deletion that does not include the breakpoint region in a child with typical facial features and truncus arteriosus and raises the question whether effort has been concentrated in the wrong region. It also draws attention back to the possible role of the transcription factor TUPLE1, which is expressed in the bronchial arches and outflow tract of the heart but which has been discounted because the encoding gene is situated far from the balanced translocation breakpoint.

18. ° Sutherland HF, Wadey R, McKie JM, Taylor C, Atif U, Johnstone KA, Halford S, Kim U, Goodship J, Baldini A, Scambler PJ: **Identification of a novel transcript disrupted by a balanced translocation asociated with DiGeorge syndrome.** *Am J Hum Genet* 1996, in press.

This is an intriguing paper detailing the identification of an alternatively spliced polyadenylated cDNA which spans the ADU breakpoint but does not appear to have any coding potential. The exons are conserved in the mouse, in which expression and alternative splicing also occurs. It remains to be seen whether this is some sort of pseudogene, which seems unlikely, or a functional RNA, which has few precedents.

19. Bleyl S, Nelson L, Odelberg SJ, Ruttenberg HD, Otterud B, Leppert M, Ward K: **A gene for familial total anomalous pulmonary venous return maps to chromosome 4p13–q12.** *Am J Hum Genet* 1995, 56:408–415.

20. Kurihara Y, Kurihara H, Oda H, Maemura K, Nagai R, Ishikawa T, Yazaki Y: **Aortic arch malformations and ventricular septal defect in mice deficient in endothelin-1.** *J Clin Invest* 1995, 96:293–300.

21. Meyer D, Birchmeier C: **Multiple essential functions of neuregulin in development.** *Nature* 1995, 378:386–390.

22. Lee KF, Simon H, Chen H, Bates B, Hung MC, Hauser C: **Requirement for neuregulin receptor erB2 in neural and cardiac development.** *Nature* 1995, 378:394–398.

23. Gassman M, Casagranda F, Orioli D, Simon H, Lai C, Klein R, Lemke G: **Aberrant neural and cardiac development in mice lacking erB4 neuregulin receptor.** *Nature* 1995, 378:390–394.

24. Shull MM, Ormsby I, Kier AB, Pawlowski S, Diehold RJ, Yin M, Allen R, Sidman C, Proetzel G, Calvin D *et al.*: **Targeted disruption of the mouse transforming growth factor β1 gene results in multifocal inflammatory disease.** *Nature* 1992, 359:693–699.

25. Letterio JJ, Geiser AG, Kulkarni AB, Roche NS, Spom MB, Roberts AB: **Maternal rescue of transforming growth factor- β1 null mice.** *Science* 1994, 264:1936–1938.

26. Threadgill DW, Dlugosz AA, Hansen LA, Tennebaum T, Lichti U, Yee D, LaMantia C, Mourton T, Herrup K, Harris RC *et al.*: **Targeted disruption of mouse EGF receptor: effect of genetic background on mutant phenotype.** *Science* 1995, 269:230–234.

27. Saga Y, Yagi T, Ikawa Y, Sakakura T, Aizawa S: **Mice develop normally without tenascin.** *Genes Dev* 1992, 6:1821–1831.

28. Yokoyama T, Copeland NG, Jenkins NA, Montgomery CA, Elder FFB, Overbeek PA: **Reversal of left–right asymmetry: a *situs inversus* mutation.** *Science* 1993, 260:679–682.

29. Yokoyama T, Harrison WR, Elder FFB, Overbeek PA: **Molecular analysis of the *Inv* insertional mutation.** In *Developmental Mechanisms of Heart Disease.* Edited by Clark EB, Markwald RR, Takao A. New York: Futura Publishing Company; 1995:513–520.

30. ° Reaume AG, De Sousa PA, Kulkarni S, Langille BL, Zhu D, Davies TC, Juneja SC, Kidder GM, Rossant J: **Cardiac malformation in neonatal mice lacking connexin43.** *Science* 1995, 267:1831–1834.

Connexin 43 is a gap junction protein that is expressed from the onset of zygotic transcription, supplying subunits for the earliest gap junctions that form in mammalian development. It is also widely expressed in embryonic and adult organs. Neonatal mice lacking *connexin 43* display enlargement of the conus region overlying the right ventricular outflow tract and, on section, this region is filled with septae rather than being an open channel.

31. ° Britz-Cunningham SH, Shah MM, Zuppan CW, Fletcher WH: **Mutations of the *Connexin43* gap-junction in patients with heart malformations and defects of laterality.** *N Engl J Med* 1995, 332:1323–1329.

On the basis of the results presented in [30•], Britz Cunningham *et al.* in this study looked for mutations in connexin 43 in the hearts from 30 children who had had cardiac transplantation. Mutations were reported in seven cases, six of these had visceroatrial heterotaxia and one had an atrial septal defect. This paper generated great excitement, but two groups have now failed to reproduce these results in much larger series of children with visceroatrial heterotaxia.

32. Casey B, Ballabio A: ***Connexin43* mutations in sporadic and familial defects of laterality.** *N Engl J Med* 1995, 333:941.

33. Penman Splitt M, Burn J, Goodship J: ***Connexin43* mutations in sporadic and familial defects of laterality [Letter].** *N Engl J Med* 1995, 333:941.

34. Winqvist R, Lundstrom K, Salminen M, Laatikainen M, Ulmanen I: **The human catechol-o-methyltransferase (COMT) gene maps to band q11.2 of chromosome 22 and shows frequent RFLP with BgII.** *Cytogenet Cell Genet* 1992, 59:253–257.

STIC-ILL

From: Chen, Shin-Lin
Sent: Friday, June 29, 2001 4:26 PM
To: STIC-ILL
Subject: article

please provide the following articles ASAP. Thanks!
Serial No. 09/258,217.

L8 ANSWER 5 OF 10 MEDLINE DUPLICATE 4
AU Faury G; Maher G M; Li D Y; Keating M T; Mecham R P; Boyle W A
TI Relation between outer and luminal diameter in cannulated arteries.
SO AMERICAN JOURNAL OF PHYSIOLOGY, (1999 Nov) 277 (5 Pt 2) H1745-53.
Journal code: 3U8; 0370511. ISSN: 0002-9513.

L8 ANSWER 9 OF 10 MEDLINE DUPLICATE 7
AU Morris C A
TI Genetic aspects of supravalvular aortic stenosis.
SO CURRENT OPINION IN CARDIOLOGY, (1998 May) 13 (3) 214-9. Ref: 56
Journal code: BDA; 8608087. ISSN: 0268-4705.
(Please provide this reference first)

L8 ANSWER 10 OF 10 MEDLINE DUPLICATE 8
AU Burn J; Goodship J
TI Developmental genetics of the heart.
SO CURRENT OPINION IN GENETICS AND DEVELOPMENT, (1996 Jun) 6 (3) 322-5. Ref: 34.

Shin-Lin Chen
AU 1633
CM1 12A15
(703)305-1678

Relation between outer and luminal diameter in cannulated arteries

GILLES FAURY,[1] GAIL M. MAHER,[2] DEAN Y. LI,[3] MARK T. KEATING,[3]
ROBERT P. MECHAM,[1] AND WALTER A. BOYLE[2]
[1]*Department of Cell Biology and Physiology and* [2]*Anesthesiology Research Unit, Washington University School of Medicine, St. Louis, Missouri 63110; and* [3]*Eccles Institute of Human Genetics, Howard Hughes Medical Institute, Salt Lake City, Utah 84112*

Faury, Gilles, Gail M. Maher, Dean Y. Li, Mark T. Keating, Robert P. Mecham, and Walter A. Boyle. Relation between outer and luminal diameter in cannulated arteries. *Am. J. Physiol.* 277 (*Heart Circ. Physiol.* 46): H1745–H1753, 1999.—Resistance in blood vessels is directly related to the inner (luminal) diameter (ID). However, ID can be difficult to measure during physiological experiments because of poor transillumination of thick-walled or tightly constricted vessels. We investigated whether the wall cross-sectional area (WCSA) in cannulated arteries is nearly constant, allowing IDs to be calculated from outer diameters (OD) using a single determination of WCSA. With the use of image analysis, OD and ID were directly measured using either transillumination or a fluorescent marker in the lumen. IDs from a variety of vessel types were calculated from WCSA at several reference pressures. Calculated IDs at all of the reference WCSA were within 5% (mean < 1%) of the corresponding measured IDs in all vessel types studied, including vessels from heterozygote elastin knockout animals. This was true over a wide range of transmural pressures, during treatment with agonists, and before and after treatment with KCN. In conclusion, WCSA remains virtually constant in cannulated vessels, allowing accurate determination of ID from OD measurement under a variety of experimental conditions.

lumen; cross-sectional area; resistance

ARTERIAL LUMEN SIZE is the fundamental parameter that determines vascular resistance and therefore blood pressure, organ blood flow, as well as cardiac work. The arterial wall presents both viscoelastic and mechanical properties, and the lumen size or inside diameter (ID) is the result of the integrated effects of transmural pressure, tethering of surrounding tissues, wall elasticity, and active responses of the vascular smooth muscle (20).

A variety of approaches have been taken to quantify the effects of physiological and pharmacological perturbations on vessel diameter. In earlier studies, large vessels (up to several centimeters in diameter) were used to study the relationship between transmural pressure and diameter utilizing pulse-wave velocity-distensibility measurements (3, 14), volume measurements as a function of transmural pressure (8, 11, 24, 28), or intraluminal saline-filled balloons with ultrasonography (30). More recently, the reactivity of small resistance arteries has been studied utilizing similar techniques (19) as well as tension-displacement measurements (22), radiological dimension measurements (10), dimension measurements utilizing photoelectric diode arrays (29) or ultrasonic echotracking devices (1, 9, 12, 33), fluorescent techniques (32), and most commonly, video-dimension analysis of transilluminated vessels (26, 34). This latter method allows diameter to be measured directly in vessels of varying sizes (25, 27) and has been utilized for studies both in vivo and in vitro.

Although vascular resistance is directly related to changes in ID, outside diameter (OD) measurements are often used because they are most easily ascertained at any intravascular pressure, and ID can be difficult to accurately measure in thick-walled or tightly constricted vessels. Biomechanical studies have shown that the blood vessel wall is minimally compressible (4, 5). Thus it has been widely assumed that the vascular wall volume is constant (16, 21, 23, 31) or that by controlling or neglecting the longitudinal extension of the vessel with pressure (8), the vessel wall cross-sectional area (WCSA) could also be considered constant (7, 10, 36). These assumptions permit calculation of the ID from OD at any pressure, assuming that at least one accurate measurement of WCSA can be made. However, the general applicability of the assumption that WCSA remains constant and that ID can thereby be determined from OD using this approach has never been rigorously assessed under a range of experimental conditions.

In the present study we have investigated whether WCSA remains constant, such that ID (and therefore vascular resistance) can be calculated directly from the OD measurement during passive and active changes in diameter. In cannulated mouse arteries, in which longitudinal extension was limited, we analyzed the relationship between measured ID and the ID calculated from OD, assuming a constant WCSA. The experiments were performed in both wild-type and elastin-mutated mice (which results in a significant difference in the vessel wall structure) (17) of two different age groups (1–3 days and 5–9 mo). Three different arteries (pulmonary, ascending aorta, and carotid artery) were used, and diameter changes were measured during both increasing and decreasing transmural pressure changes (from 0 to 175 mmHg) and during active contraction and relaxation (at a constant pressure) induced by the α-adrenergic agonist phenylephrine and the endothelium-dependent vasodilator acetylcholine. These experiments were performed before and after vascular smooth

The costs of publication of this article were defrayed in part by the payment of page charges. The article must therefore be hereby marked "*advertisement*" in accordance with 18 U.S.C. Section 1734 solely to indicate this fact.

muscle and endothelial cell responses were abolished by KCN treatment. Additionally, to determine the applicability of this technique to small resistance-sized arteries, measured and calculated ID values were compared in small (~120 μm ID) mesenteric arteries during active vasoconstriction with the α-adrenergic agonist norepinephrine. Finally, we analyzed vessel dimension measurements reported in the literature (25, 30) to assess the relationship between measured and calculated ID in prior studies.

MATERIALS AND METHODS

Animals. Nine 5- to 9-mo-old and two 1- to 3-day-old C57B1/6J mice, as well as two 5- to 9-mo-old C57B1/6J mice in which one allele of the elastin gene exhibits a deletion in exon 1 (ELN +/− animals) have been studied. This deletion was shown to lead to structural and functional differences in the wall of elastic arteries (17). Housing and surgical procedures were in accordance with institutional guidelines.

Surgical procedure and mounting of vessel. The animals were anesthetized by intraperitoneal injection of pentobarbital sodium (60 mg/kg). The vessel (ascending aorta, left carotid artery, superior mesenteric artery, or left pulmonary artery) was quickly excised and placed in a physiological buffer (pH 7.4) of the following composition (mM): 135 NaCl, 5 KCl, 1.6 $CaCl_2$, 1.17 $MgSO_4$, 0.44 KH_2PO_4, 2.6 $NaHCO_3$, 0.34 Na_2HPO_4, 5.5 D-glucose, 0.025 EDTA, and 10 HEPES. The vessel was cleaned of adhering connective tissue and fat and then cannulated and mounted onto a pressure arteriograph (Living Systems Instrumentation, Burlington, VT), as previously described (2, 26). The experiments were performed in an organ bath filled with physiological buffer at 37°C. The bath was placed on an inverted microscope, and a computerized image analysis system was used for measurement of ID and OD in the transilluminated vessels as previously described (2). A digital image was used for analysis with this system, and the inherent error in any measurement was therefore ±1 pixel. This corresponded to an intrinsic error of ±1–2% of the measured ID and OD values.

Experimental protocol. In the ascending aortas and carotid arteries, following a 30-min equilibration period, intravascular (transmural) pressure was increased from 0 to 175 mmHg by steps of 25 mmHg (at least 1 min per step) and then symmetrically decreased (following the same steps and timing) back to 0 mmHg. ID and OD were recorded continuously. Integrity of smooth muscle function was assessed by bath application of the α-adrenergic vasoconstrictor phenylephrine (PE, 10^{-5} M) and endothelial cell integrity was tested by the addition of the endothelium-dependent vasodilator ACh (10^{-5} M). These latter studies were done at a constant pressure of 75 mmHg in systemic arteries or 20 mmHg in pulmonary arteries. The vessel was then treated with KCN (13 mM) in physiological buffer for 45–60 min (at 0 mmHg) to abolish smooth muscle and endothelial cell function as verified by the subsequent lack of response to PE. The response to increases (0→175 mmHg) and decreases (175→0 mmHg) in pressure was then retested after KCN treatment. The procedure was identical when using the pulmonary arteries except that the intravascular pressure range was 2–50 mmHg, by steps of 10 mmHg (except for the first step which was 2–10 mmHg). A starting pressure of 2 mmHg was necessary in the thin pulmonary vessels to maintain the cylinder shape, since these vessels tend to collapse at 0 mmHg. For each vessel type studied, all experiments were performed in at least two separate vessels: 2 newborn left pulmonary arteries, 2 adult left pulmonary arteries, 4 adult left carotid arteries, 2 adult wild-type ascending aortas, and 2 elastin-mutated ascending aortas. In addition, to assess the accuracy of the ID calculations in resistance arteries during active (i.e., agonist-induced) vasoconstriction, three small mesenteric artery segments (from two separate animals) were studied at constant pressure (40 mmHg) before and after treatment with norepinephrine (NE, 10^{-5} M) and NE + ACh (10^{-5} M).

Measurements in ascending aorta. In larger arteries, the vessel wall is often too thick to allow the edge corresponding to the ID to be visualized accurately by transillumination. This is most often a problem at lower transmural pressures (0–100 mmHg) because passive thinning of the vessel wall with increases in diameter usually allows measurement of ID by transillumination at higher pressures (125–175 mmHg). The carotid artery was variable in this regard because direct measurement of ID by transillumination across the whole pressure range (0–175 mmHg) was possible in some carotid arteries but not in others. We describe measurements performed by transillumination of carotid arteries only in arteries where we could easily detect ID by image analysis at any pressure. The wall of the ascending aorta was always too thick to allow direct ID measurement by transillumination across the lower pressure range. To measure the ID of the ascending aorta over the entire range of pressures, we filled the vessel lumen with buffer containing 25 mg/ml dextran-coupled FITC (FITC-dextran, molecular mass ≈ 500 kDa). The large size of FITC-dextran prevents it from crossing the vessel wall (32), and it therefore remains in the lumen throughout the experiment. The FITC was excited (at 420–450 nm), and ID was determined from the resulting FITC-dextran epifluorescence signal (>520 nm) corresponding to the vessel lumen by image analysis. To calibrate the ID obtained by the FITC method, the edge of the epifluorescence signal was adjusted (by adjusting the detection threshold) so that the ID measured by both transillumination and epifluorescence at 175 mmHg (where both could be measured) were identical.

Calculated ID from vessel ring wall thickness. In two carotid arteries and two ascending aortas, IDs were directly measured by transillumination or the FITC method, respectively, as described above. In addition, at the end of the experiment, wall thickness was directly measured using image analysis of a cross section (ring) of the studied vessel, which was simply cut and measured using the image analysis system. Subtracting twice the measured wall thickness of the ring from the measured OD at 0 mmHg provided another direct measurement of ID at 0 mmHg. The ID determined by this method was compared with directly measured ID using transillumination or the FITC method and was then used to calculate ID values throughout the pressure range studied. These calculated ID values were then compared with the measured ID values obtained by transillumination or the FITC method.

Calculated ID from direct measurement of WCSA by transillumination in deeply constricted mesenteric arteries. In the small mesenteric arteries, pressure was maintained at a constant level (40 mmHg), and IDs were directly measured by transillumination, as described above, before and after addition of the vasoconstrictor NE (10^{-5} M) followed by the addition of the endothelium-dependent vasodilator ACh (10^{-5} M). IDs directly measured during application of NE and ACh were then compared with IDs that were calculated using the

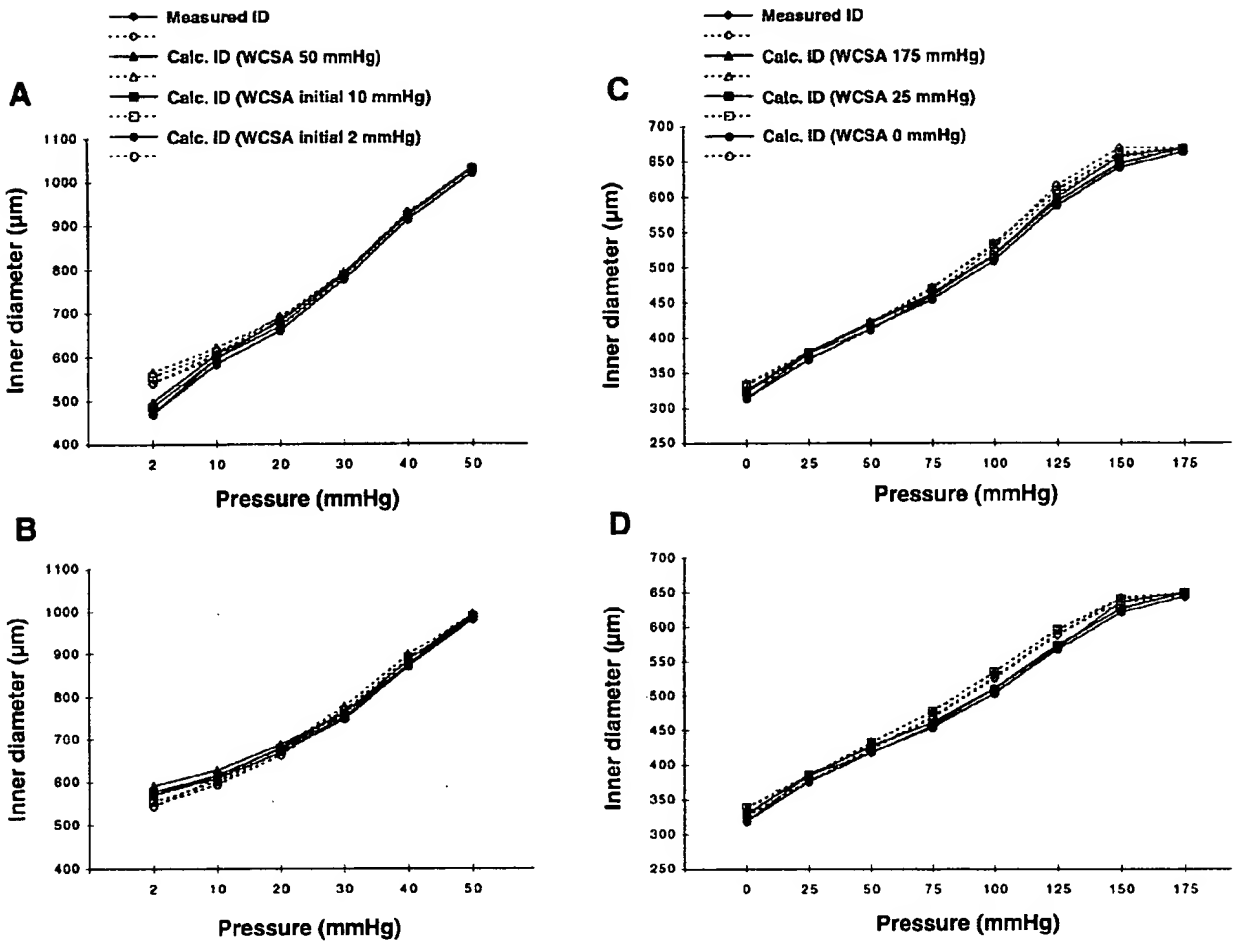

Fig. 1. Relation between measured inner diameter (ID) and calculated ID in adult mouse pulmonary and carotid arteries. Figure is based on results from a single left pulmonary artery before (*A*) and after (*B*) treatment with KCN and on a single carotid artery before (*C*) and after (*D*) treatment with KCN. Results are representative of the results obtained in 2 separate pulmonary arteries and 4 separate carotid arteries. Solid lines, increasing pressure phase; dotted lines, decreasing pressure phase. Calc. ID (WCSA*y* mmHg, where *y* represents the pressure value), calculated ID from vessel wall cross-sectional area at *y* mmHg.

WCSA value obtained from direct ID and OD measurement at 40 mmHg (before addition of vasoactive agents).

Chemicals. All the chemicals were obtained from Sigma Chemical (St. Louis, MO), except NaCl, which was obtained from Fisher Scientific (St. Louis, MO).

Analysis of previously published data. OD and ID values of vessels were derived directly from the processed data presented in the articles cited using the corresponding transformation formulas given by the authors. The calculated and measured ID values were then analyzed and compared using the same methods as those used for the other experiments reported here.

Because of the inherently large error in the measured and calculated ID values at 0 mmHg (and 2 mmHg in the pulmonary artery), these values were excluded from the error ranges and mean errors reported in this paper (see DISCUSSION).

Analysis of relation between OD and ID. For each vessel, the ID was calculated at each pressure step (P*x*) based on the measured OD at the same pressure and on the WCSA at a reference pressure (P*y*), with the assumptions that WCSA was constant and that the vessel was a perfect cylinder. The formulas used were as follows

$$\mathrm{WCSA} = \pi \mathrm{OD}^2/4 - \pi \mathrm{ID}^2/4 = \pi/4(\mathrm{OD}^2 - \mathrm{ID}^2) \quad (1)$$

$$\mathrm{WCSA}_{Px} = \mathrm{WCSA}_{Py} \quad (2)$$

$$\mathrm{OD}^2_{Px} - \mathrm{ID}^2_{Px} = \mathrm{OD}^2_{Py} - \mathrm{ID}^2_{Py} \quad (3)$$

$$\mathrm{ID}_{Px} = \sqrt{(\mathrm{OD}^2_{Px} - \mathrm{OD}^2_{Py} + \mathrm{ID}^2_{Py})} \quad (4)$$

These formulas permit ID at any pressure (ID_{Px}) to be calculated from the measured OD at that pressure (OD_{Px}) assuming a constant WCSA, which has been calculated from a direct measurement of both ID (ID_{Py}) and OD (OD_{Py}) at some reference pressure (P*y*). To verify the general applicability of this approach, we determined reference WCSA (WCSA_{Py}) at five reference pressures (P*y*): 0, 25, and 175 mmHg as the pressure was raised, and 25 and 0 mmHg as the pressure was

lowered in the systemic vessels; and 2, 10, and 50 mmHg as the pressure was raised, and 2 and 10 mmHg as the pressure was lowered in the pulmonary vessels. For the small mesenteric arteries, the reference WCSA was calculated at 40 mmHg.

In the analysis of the data from the literature, $WCSA_{Py}$ was calculated at 0, 25, and 125 mmHg for the data published by Osol and Cipolla (25) and 0, 5, 25, 190 mmHg for the data published by Storkholm et al. (30).

The calculated ID (ID_c) and measured ID (ID_m) were compared at each pressure step, and percent error (E) was calculated as

$$E = 100(ID_c - ID_m)/ID_m \quad (5)$$

RESULTS

Adult mouse left pulmonary artery. The measured versus calculated ID values obtained from one adult pulmonary artery are shown before (Fig. 1*A*) and after treatment with KCN (Fig. 1*B*). The ID data obtained during pressure increases (solid lines) and decreases (dotted lines) from 2 to 50 mmHg are shown. As can be seen in Fig. 1, the measured ID and calculated ID using WCSA references at 2, 10, and 50 mmHg are nearly identical. Including the values from the two separate vessels studied, at all five of the reference WCSAs tested (both before and after treatment with KCN), the mean error (168 calculated ID values) was −0.63% with an error value range of −3.7% to +2.4%. Of these calculated values, 90% (151 of 168) were within an error range of −2.1% to +2.1%.

Adult mouse left carotid artery. In Fig. 1, *C* and *D*, the measured versus calculated ID values obtained from the adult carotid artery are shown before and after KCN treatment, respectively. For these experiments, ID was studied during pressure increases (solid lines) and decreases (dotted lines) from 0 to 175 mmHg. Again, the measured ID and calculated ID values are nearly identical at each WCSA reference shown in Fig. 1 (0, 25, and 175 mmHg). Including the values from the four separate vessels, at all five of the reference WCSAs studied (both before and after KCN), the mean error (496 calculated ID values) was −0.89% with an error value range of −4.9% to +4.9%. Of these calculated values, 90% (446 of 496) were within an error range of −3.2% to +3.2%.

Newborn mouse left pulmonary artery. The difference between measured ID and calculated ID was again quite low in the newborn pulmonary artery (Fig. 2). This was true at all pressures tested (2–50 mmHg), whether pressure was increasing (solid lines) or decreasing (dotted lines), using any of the five reference WCSAs before and after treatment with KCN. Including values from the two separate vessels studied, the mean error (168 calculated ID values) was +0.1% with a error value range of −4.8% to +2.9%. Moreover, >90% (151 of 168) of these calculated values were within an error range of −1.6% to +1.6%.

Adult mouse ascending aorta. As shown in Fig. 3, some differences in size and response to pressure changes were observed between vessels from elastin-deficient (ELN +/−) and wild-type animals, but the

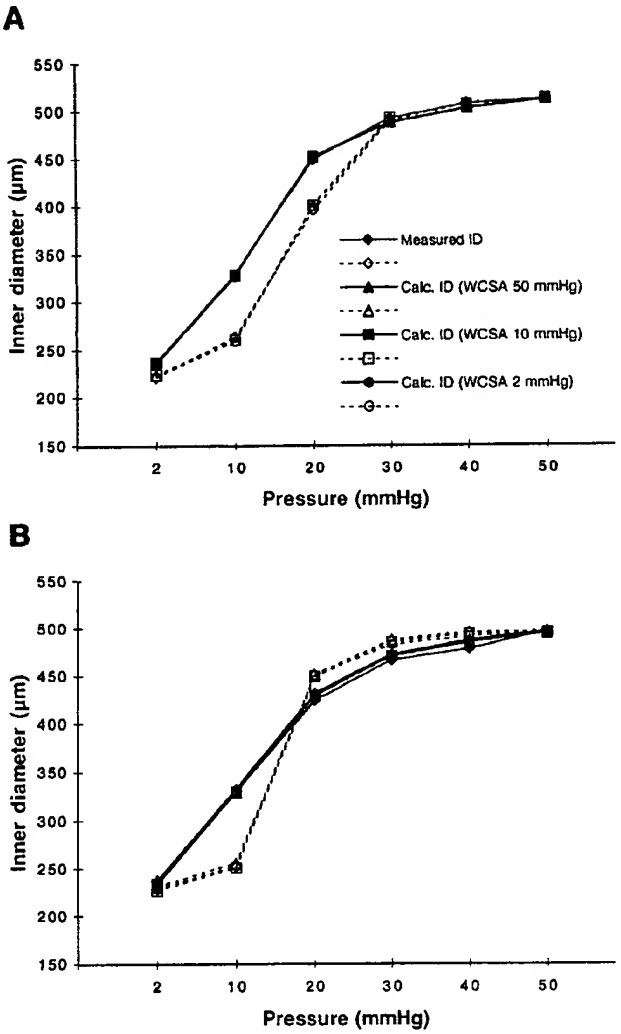

Fig. 2. Relation between measured ID and calculated ID in newborn mouse pulmonary artery. Results shown are from a single left pulmonary artery before (*A*) and after (*B*) treatment with KCN and are a representative example of the results obtained in 2 separate vessels. Solid lines, increasing pressure phase; dotted lines, decreasing pressure phase.

difference between measured ID and calculated ID was again quite low in the ascending aorta from both animals. For all five reference WCSAs studied in the four separate vessels tested (two wild-type and two ELN +/−), both before and after KCN (496 calculated ID values), the mean error was +0.32% with a range of −4.2% to +4.6%. Moreover, >90% (446 of 496) of these calculated values were within an error range of −2.7% to +2.7%.

Action of vasoactive agents on vessels. The effects of active contraction and relaxation of the vessel wall on differences between measured and calculated ID were studied utilizing the vasoconstricting agonist PE (10^{-5} M) followed by the addition of the endothelium-dependent vasorelaxing agent ACh (PE + ACh, 10^{-5} M). In Fig. 4, where the response of a single representa-

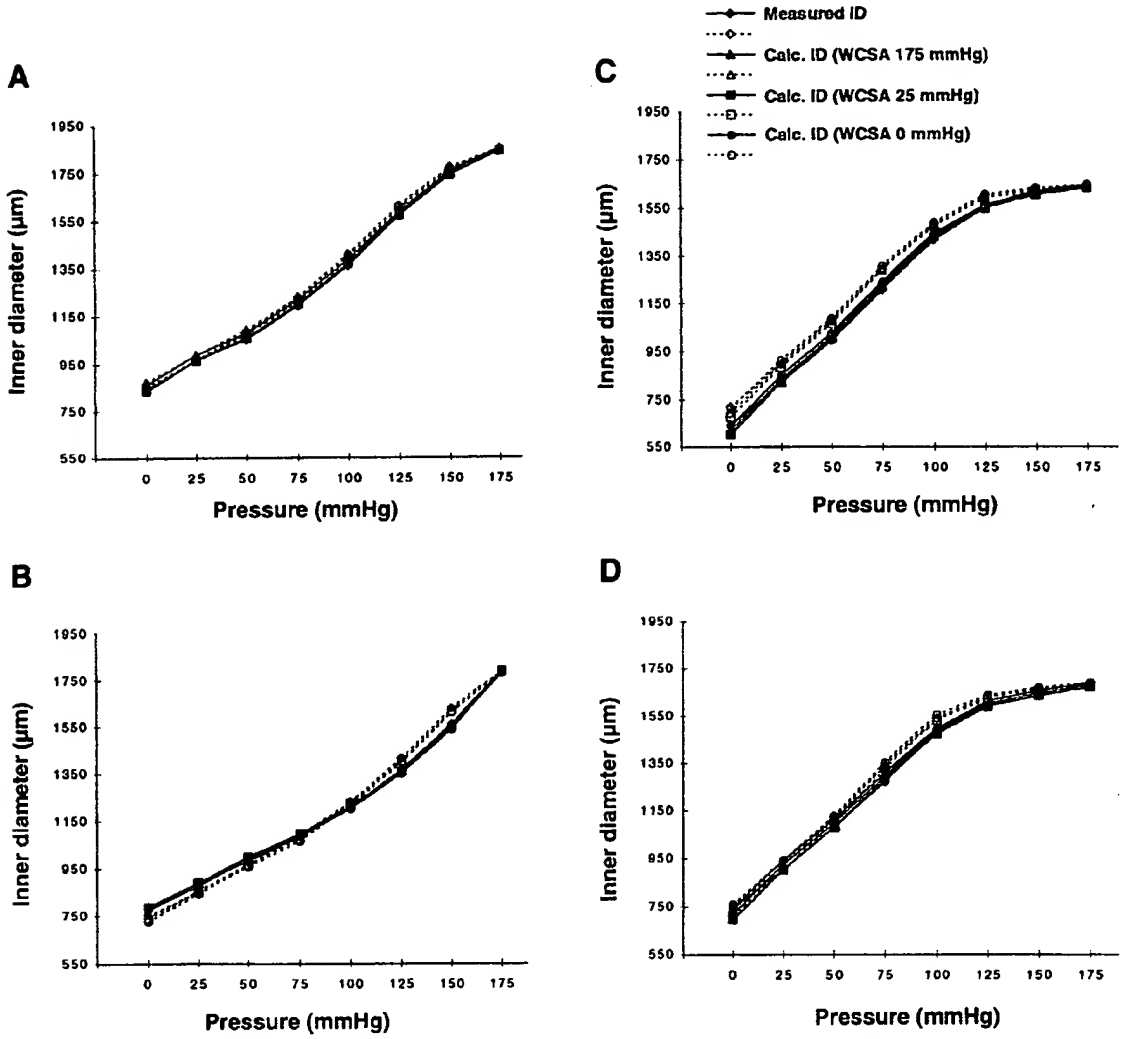

Fig. 3. Relation between measured ID and calculated ID in the adult mouse ascending aorta. Figure is based on results from a single wild-type ascending aorta before (*A*) and after (*B*) treatment with KCN and on a single heterozygous elastin-mutated ascending aorta before (*C*) and after (*D*) treatment with KCN. Results are representative examples of the results obtained in 2 separate wild-type and 2 separate elastin-mutated ascending aortas. Solid lines, increasing pressure phase; dotted lines, decreasing pressure phase.

tive vessel for each vessel type is presented, the measured ID values for each treatment are shown together with the calculated ID values, utilizing the WCSA reference at each of the pressures indicated. Again, there is little difference between the measured ID and the calculated ID during these treatments using WCSA at any of the reference pressures. Pooling the data from all 12 vessels used (2 newborn pulmonary arteries, 2 adult pulmonary arteries, 4 carotid arteries, 2 wild-type ascending aortas, and 2 ELN+/− ascending aortas) before and after treatment with PE or PE + ACh, the mean error (180 calculated ID values) was −0.12% with a range of −4.4% to +4.9%. Moreover, >90% (162 of 180) of these calculated values were within an error range of −3.4% to +3.4%.

There was no evidence of light-dye injury of smooth muscle cells or endothelial cells in microvessels, despite the use of a higher concentration of FITC-dextran than previously reported (6, 32). The large elastic arteries studied here by the FITC method still responded well to the vasoconstricting and the endothelium-dependent vasodilator agonists (Fig. 4). Comparison of ascending aorta ODs with FITC filling (n = 5) to ascending aorta ODs previously studied in the same conditions without FITC filling (n = 15) showed no significant differences (by 2-way ANOVA) in PE-induced vasoconstriction or ACh-induced dilation before and after FITC. PE-induced vasoconstriction resulted in 17 ± 4% and 21 ± 2% decreases in OD with and without FITC, respectively; ACh relaxed the PE-constricted vessels by 75 ± 16% and 85 ± 9% with and without FITC, respectively.

In the small mesenteric arteries, IDs were directly measured by transillumination at a constant transmural pressure of 40 mmHg before and after addition of

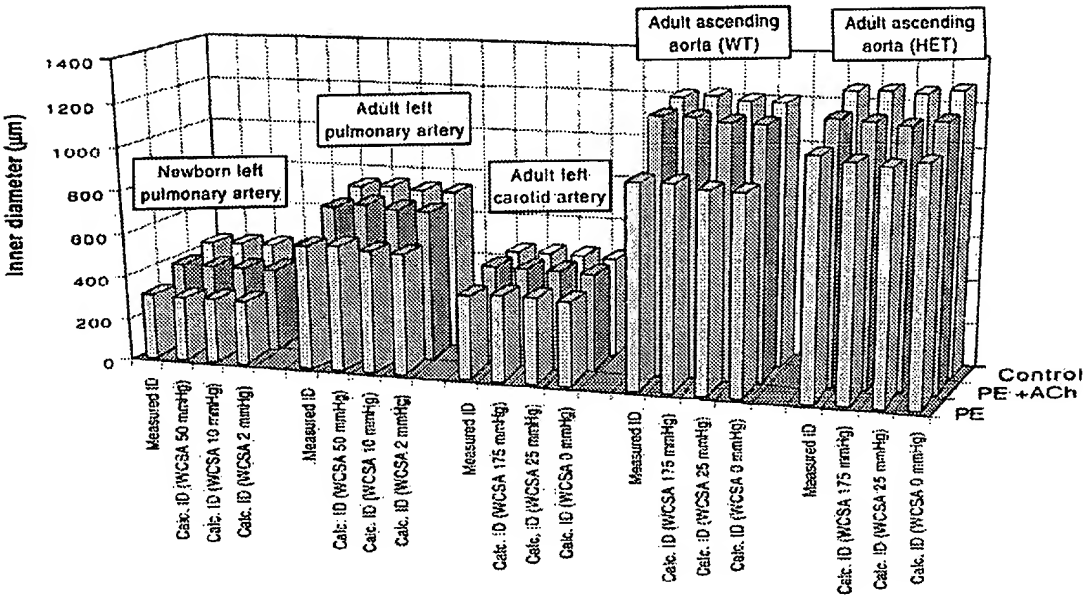

Fig. 4. Effect of vasoactive agents on the relation between measured ID and calculated ID. Figure is based on results from a single vessel of each type. Similar results were obtained from 2 separate newborn pulmonary arteries, 2 separate adult pulmonary arteries, 4 separate adult carotid arteries, and from 2 separate wild-type (WT) and 2 separate elastin-mutated adult ascending (HET) aortas. Control transmural pressure was 75 mmHg in systemic vessels and 20 mmHg in pulmonary vessels. Phenylephrine (PE) and acetylcholine (ACh) concentrations were 10^{-5} M.

the vasoconstrictor NE (10^{-5} M) and ACh (NE + ACh, 10^{-5} M). ID values calculated from the WCSA derived from the measured ID and OD before any treatment (at 40 mmHg) were then compared with the directly measured values (Fig. 5). Again, very little difference was found between directly measured IDs and calculated IDs. With the data from all three vessel segments used pooled together, before and after treatment with NE and NE + ACh, the mean error (6 calculated ID values) was −1.3% with a range of −3.5% to +1.0%.

Calculated ID from vessel ring wall thickness. In some vessels or some experimental conditions it may not be possible to accurately measure ID and calculate a reference WCSA. Thus we investigated whether ID determined from wall thickness of a cut ring segment at the end of an experiment (see MATERIALS AND METHODS), together with measured OD at 0 mmHg (in the cannulated vessel), could be used to accurately calculate a reference WCSA that could then be used post hoc to calculate ID from OD. In the carotid arteries studied the IDs determined from measurement of the ring wall thickness were 329 and 264 μm, respectively, consistent with the measured IDs (by transillumination) of 325 and 258 μm. Similarly, the IDs in the ascending aorta ring cross sections of 781 μm for the wild-type animal and 732 μm for the mutant animal were similar to the directly measured IDs of 751 and 754 μm, respectively, using the FITC method. In all cases, the differences are in the range of one pixel, supporting the accuracy of ID measurements by all three methods (transillumination, FITC, and cross-section analysis). As shown in Fig. 6, there was little difference in the ID values calculated from the ring cross sections and in the respective ID values obtained by direct measurement in the carotid artery by transillumination (Fig. 6, *A* and *C*), or in the ascending aorta by the FITC method

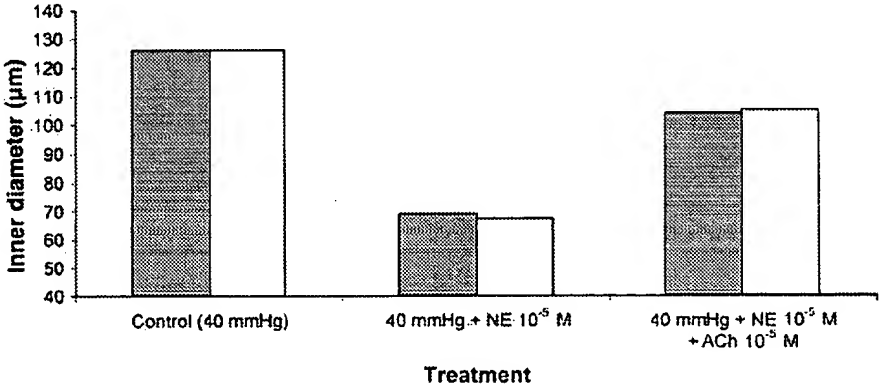

Fig. 5. Relation between measured ID and calculated ID from norepinephrine (NE)-constricted and ACh-relaxed small mesenteric artery segments. Figure is based on results from a single segment of the adult mesenteric artery, with similar results obtained in 3 separate artery segments. Solid bars, measured ID from direct measurement by transillumination. Open bars, calculated IDs from vessel wall cross-sectional area.

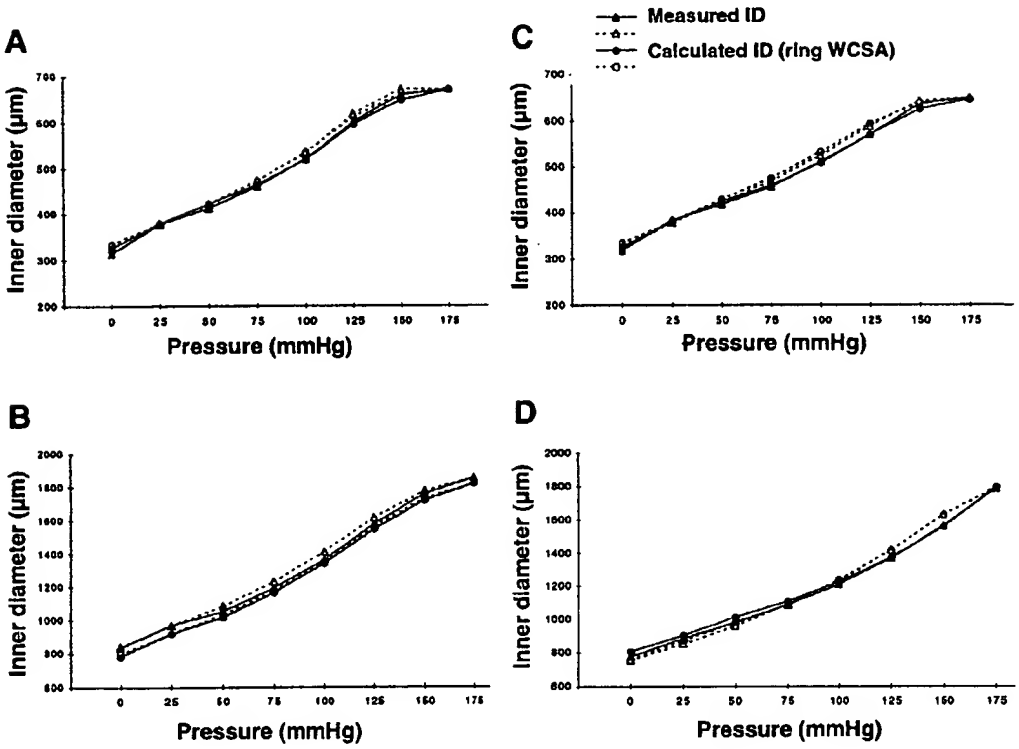

Fig. 6. Relation between measured ID and calculated ID from a measurement of wall thickness in a cross section of vessel. Figure is based on results from a single adult mouse carotid artery before (*A*) and after (*C*) KCN treatment and on a single adult mouse ascending aorta before (*B*) and after (*D*) KCN treatment. Results are representative of those obtained in 2 separate adult ascending aortas (wild-type and elastin mutated) and 2 separate adult carotid arteries. Solid lines, increasing pressure phase; dotted lines, decreasing pressure phase.

(Fig. 6, *B* and *D*), both before and after KCN treatment. The measurements in the two carotid arteries (52 independent ID measurements) had a mean error of −0.4% with an error range of −3.9% to +4.6%. Of these calculated error values, 90% (47 of 52) were within a range of −3.7% to +3.7%. For the two ascending aortas (52 independent ID measurements) the mean error was +0.2% with a range of −5.0% to +5.7%, with 90% (47 of 52) of these calculated values within an error range of −4.6% to +4.6%.

DISCUSSION

Vascular resistance and associated physiological parameters are directly related to the diameter of the vessel lumen, but ID is often difficult to measure directly in intact blood vessels. As a result, many investigators have calculated ID from OD in pressurized blood vessels based on the assumption that the vessel wall volume or WCSA is constant (7, 10, 16, 21, 23, 31, 36). However, these assumptions have never been rigorously tested in physiological conditions. Our hypothesis was that a constant wall volume would result in a nearly constant WCSA under conditions in which longitudinal extension of cannulated arteries is restricted by the experimental device. This is similar to the situation in vivo where longitudinal extension of vessels is limited by the tethering of surrounding tissue. In the studies presented here, the constant relationship between OD and ID under these conditions, on the basis of the assumption of constant WCSA, was demonstrated in a wide range of physiological situations in transilluminated, pressurized, cannulated vessels from a variety of sources.

In all the vessels investigated, including arteries from elastin-deficient mice, under conditions where pressure was increasing or decreasing, during active contraction and relaxation, or following treatment with KCN, the difference between calculated ID and measured ID was always quite low, with mean errors generally <1%. This indicates that WCSA is relatively constant, in agreement with a prior study of WCSA during changes in flow and during NE-induced contraction in rat mesenteric arteries (15). Our data demonstrate that this can be applied to both large conductance (Figs. 1–4) and small resistance arteries (Fig. 5). With the use of this technique, ID and vascular resistance can be closely approximated in tightly constricted or thick-walled arteries in which the lumen size (ID) cannot be determined from visual inspection.

We did note some differences in the accuracy of calculated ID that depended on the pressure level at which the reference WCSA was measured. In particular, larger differences between calculated and measured ID were consistently found for IDs at 0 mmHg. Similarly, when WCSA at 0 mmHg was used as the reference to calculate ID, the differences between calcu-

lated and measured ID were larger than those obtained when a reference WCSA at a higher pressure was used. This slight discontinuity in the relation between calculated ID and measured ID between the unpressurized (i.e., 0 mmHg) and pressurized vessels is not surprising. Previous observations have demonstrated that the elastic structures of the vascular wall, including the intima, decrease in size, infold, and bulge in the collapsed vessel as intravascular pressure decreases to 0 mmHg (13, 35). Nevertheless, the differences between measured and calculated ID remained quite small, even when the reference WSCA at 0 mmHg was derived from the wall thickness at the end of the experiment (Fig. 6).

In addition to our experiments, we analyzed data from the literature where our hypothesis could also be tested (Table 1). Analyses of the diameter measurements made by Osol and Cipolla (25) in small rat uteroplacental arteries and the analysis of the data from porcine aorta made by Storkholm et al. (30) are presented in Table 1. The data shown in Table 1 include both the measured ID values (derived from the reported data) and the calculated ID values (derived from measured OD and WCSA at the pressures indicated) and the error range and mean error for the calculated values. When initially evaluating these data, it was again clear that the calculated ID values at 0 mmHg again had consistently higher errors than the calculated ID values at other pressures, presumably due to the same instability in the circular shape of the vessel at 0 mmHg as discussed above. As done elsewhere in the paper, the error values at 0–2 mmHg were thus excluded from the error ranges and means shown. Excluding these measurements (at 0 mmHg), only a few outlier error measurements >5% are evident in the raw error measurements, and mean errors varied between −4.1% and +3.4%, with the exception of one value of 7.2% in which the reference WCSA at 0 mmHg was used. The results from the literature thus lend further support to the validity of this method for calculating ID from OD measurements.

Until now, measurement of ID in cannulated arteries by transillumination has been the preferred method, but this technique is applicable to only thin-walled vessels and may even be difficult in these vessels during active contraction (18, 26). In large thick-walled arteries, direct ID measurements are often not possible because of the inability to obtain an adequately contrasted image with transillumination. Our results suggest that the FITC method can be used to measure ID in such vessels, but the fluorescence may lead to light-dye damage (6, 32), and this method still requires

Table 1. *Analysis of data from the literature*

	Pressure, mmHg									Error Range, %*		Mean Error, %*
	0	25	50	75	100	125				Minimum	Maximum	
Rat uteroplacental artery (nonpregnant)												
Measured ID, μm	78.0	117.0	142.0	152.0	156.0	158.0						
Calculated ID (from WCSA@125 mmHg), μm	93.4	127.0	147.8	153.6	155.8							
% Error	19.7	8.5	4.1	1.0	−0.1					−0.1	8.5	3.4
Calculated ID (from WCSA@25 mmHg), μm	79.3		139.3	145.4	147.8	150.1						
% Error	1.6		−1.9	−4.3	−5.2	−5.0				−5.2	−1.9	−4.1
Calculated ID (from WCSA@0 mmHg), μm		116.1	138.6	144.7	147.1	149.4						
% Error		−0.7	−2.4	−4.8	−5.7	−5.4				−5.7	−0.7	−3.8
Rat uteroplacental artery (late pregnant)												
Measured ID, μm	109.0	195.0	230.0	234.0	239.0	243.0						
Calculated ID (from WCSA@125 mmHg), μm	126.2	202.2	231.8	235.9	239.5							
% Error	15.8	3.7	0.8	0.8	0.2					0.2	3.7	1.4
Calculated ID (from WCSA@25 mmHg), μm	114.2		225.5	229.8	233.5	237.0						
% Error	4.8		−2.0	−1.8	−2.3	−2.5				−2.5	−1.8	−2.2
Calculated ID (from WCSA@0 mmHg), μm		192.0	222.9	227.2	230.9	234.5						
% Error		−1.6	−3.1	−2.9	−3.4	−3.5				−3.5	−1.6	−2.9
Pressure, mmHg	0	5	25	50	75	112.5	133	150	190			
Abdominal porcine aorta												
Measured ID, mm	7.3	7.6	8.2	9.3	10.3	10.9	11.2	11.5	11.7			
Calculated ID (from WCSA@190 mmHg), mm	8.3	7.6	8.2	9.4	10.4	11.1	11.3	11.5				
% Error	12.9	0.9	0.4	1.5	1.4	2.3	0.9	−0.1		−0.1	2.3	1.0
Calculated ID (from WCSA@25 mmHg), mm	8.2	7.6		9.4	10.4	11.1	11.3	11.5	11.7			
% Error	12.5	0.4		1.2	1.2	2.1	0.7	−0.3	−0.2	−0.3	2.1	0.7
Calculated ID (from WCSA@5 mmHg), mm	8.2		8.2	9.4	10.4	11.1	11.3	11.5	11.6			
% Error	12.1		−0.4	0.9	1.0	1.9	0.5	−0.4	−0.4	−0.4	1.9	0.4
Calculated ID (from WCSA@0 mmHg), mm		6.6	7.3	8.6	9.7	10.4	10.7	10.8	11.0			
% Error		−12.8	−11.1	−7.3	−5.7	−4.0	−5.1	−5.8	−5.5	−12.8	−4.0	−7.2

Relation between measured inner diameter (ID) and calculated ID in the rat uteroplacental artery and in the abdominal porcine aorta. Rat uteroplacental artery in nonpregnant animals and late-pregnant animals from original measurements by Osol and Cipolla (25). Abdominal porcine aorta from original measurements by Storkholm et al. (30). WCSA; wall cross-sectional area; % Error = (calculated ID/measured ID − 1) × 100. * Excludes values at 0 mmHg.

calibration with at least one accurate ID measurement. Alternatively, our data indicate that ID can be accurately estimated from OD values retrospectively, utilizing the wall thickness determined on a cut section of the vessel at the end of the experiment. The simple approach presented here for determining ID and related physiological parameters (e.g., vascular resistance) from the measured OD should prove particularly useful for both in vivo and in vitro studies of vascular reactivity and mechanics.

We thank D. Taylor and Dr. L. Parvathaneni for technical assistance

This work was supported by postdoctoral fellowships (to G. Faury) from the Fondation pour la Recherche Médicale (France), from the American Heart Association, Missouri Affiliate, and National Institute of General Medical Sciences Grant GM-55849 (to W. A. Boyle), and from National Heart, Lung, and Blood Institute Grants HL-53325 and HL-61006 (to R. P. Meham).

Address for reprint requests and other correspondence: R. P. Mecham, Dept. of Cell Biology and Physiology, 660 South Euclid Ave., Washington Univ. School of Medicine, St. Louis, MO 63110 (E-mail: bmecham@cellbio.wustl.edu).

Received 6 April 1998; accepted in final form 28 May 1999.

REFERENCES

1. **Boutouyrie, P., Y. Bézie, P. Lacolley, P. Challande, P. Chamiot-Clerc, A. Benetos, J. F. R. de la Faverie, M. Safar, and S. Laurent.** In vivo/in vitro comparison of rat abdominal aorta wall viscosity. Influence of endothelial function. *Arterioscler. Thromb. Vasc. Biol.* 17: 1346–1355, 1997.
2. **Boyle, W. A. III, and G. M. Maher.** Endothelium-independent vasoconstricting and vasodilating actions of halothane on rat mesenteric resistance blood vessels. *Anesthesiology* 82: 221–235, 1995
3. **Bramwell, J. C., A. C. Downing, and A. V. Hill.** The effect of blood pressure on the extensibility of the human artery. *Heart* 10: 289–300, 1923.
4. **Carew, T. E., R. N. Vaishnav, and D. J. Patel.** Compressibility of the arterial wall. *Circ. Res.* 23: 61–68, 1968.
5. **Chuong, C. J., and Y. C. Fung.** Compressibility and constitutive equation of arterial wall in radial compression experiments. *J. Biomech.* 17: 35–40, 1984.
6. **Damon, D. H., and B. R. Duling.** Distribution of capillary blood flow in the microcirculation of the hamster: an in vivo study using epifluorescent microscopy. *Microvasc. Res.* 27: 81–95, 1984.
7. **Davison, I. G., G. M. Wright, and M. E. DeMont.** The structure and physical properties of invertebrate and primitive vertebrate arteries. *J. Exp. Biol.* 198: 2185–2196, 1995.
8. **Fenn, W. O.** Changes in length of blood vessels on inflation. In: *Tissue Elasticity*, edited by J. W. Remington. Washington, D.C.: Am. Physiol. Soc., 1957, p. 154–167.
9. **Gamble, G., J. Zorn, G. Sanders, S. MacMahon, and N. Sharpe.** Estimation of arterial stiffness, compliance, and distensibility from M-mode ultrasound measurements of the common carotid artery. *Stroke* 25: 11–16, 1994.
10. **Greenwald, S. E., C. L. Berry, and S. G. Haworth.** Changes in the distensibility of the intrapulmonary arteries in the normal newborn and growing pig. *Cardiovasc. Res.* 16: 716–725, 1982.
11. **Hallock, P., and I. C. Benson.** Studies on the elastic properties of human isolated aorta. *J. Clin. Invest.* 16: 595–602, 1937.
12. **Hayoz, D., Y. Tardy, F. Perret, B. Waeber, J. J. Meister, and H. R. Brunner.** Non-invasive determination of arterial diameter and distensibility by echo-tracking techniques in hypertension. *J. Hypertens.* 10, *Suppl.* 5: S95–S100, 1992.
13. **Kessel, R. G., and R. H. Kardon.** *Tissues and Organs: A Text Atlas of Scanning Electron Microscopy.* San Francisco, CA: Freeman, 1979, p. 35–50.
14. **Landowne, M.** Pulse wave velocity as an index of arterial elastic characteristics. In: *Tissue Elasticity*, edited by J. W. Remington. Washington, D.C.: Am. Physiol. Soc., 1957, p. 168–176.
15. **Lee, R. M. K. W., J. B. Forrest, R. E. Garfield, and E. E. Daniel.** Comparison of blood vessel wall dimensions in normotensive and hypertensive rats by histometric and morphometric methods. *Blood Vessels* 20: 245–254, 1983.
16. **Lew, M. J., and J. A. Angus.** Wall thickness to lumen diameter ratios of arteries from SHR and WKY: comparison of pressurized and wire-mounted preparations. *J. Vasc. Res.* 29: 435–442, 1992.
17. **Li, D. Y., G. Faury, D. G. Taylor, E. C. Davis, W. A. Boyle, R. P. Mecham, P. Stenzel, B. Boak, and M. T. Keating.** Novel arterial pathology in mice and humans hemizygous for elastin. *J. Clin. Invest.* 102: 1783–1787, 1998.
18. **Mackey, K., M. C. Meyer, W. S. Stirewalt, B. C. Starcher, and M. K. McLaughlin.** Composition and mechanics of mesenteric resistance arteries from pregnant rats. *Am. J. Physiol.* 263 (*Regulatory Integrative Comp. Physiol.* 32): R2–R8, 1992.
19. **Michel, J. B., D. Heudes, O. Michel, P. Poitevin, M. Philippe, E. Scalbert, B. Corman, and B. I. Levy.** Effect of chronic ANG I-converting enzyme inhibition on aging processes. II. Large arteries. *Am. J. Physiol.* 267 (*Regulatory Integrative Comp. Physiol.* 36): R124–R135, 1994.
20. **Milnor, W. R.** *Cardiovascular Physiology.* New York: Oxford University Press, 1990.
21. **Monos, E., and A. G. B. Kovách.** Effect of acute ischaemia on active and passive large deformation mechanics of canine carotid arteries. *Acta Physiol. Acad. Sci. Hung.* 54: 23–31, 1979.
22. **Mulvany, M. J., and W. Halpern.** Contractile properties of small arterial resistance vessels in spontaneously hypertensive and normotensive rats. *Circ. Res.* 41: 19–26, 1977.
23. **Nagasawa, S., H. Handa, Y. Naruo, K. Moritake, and K. Hayashi.** Experimental cerebral vasospasm arterial wall mechanics and connective tissue composition. *Stroke* 13: 595–600, 1982.
24. **Nichol, J. T.** The effect of cholesterol feeding on the distensibility of the isolated thoracic aorta of the rabbit. *Can. J. Biochem. Physiol.* 33: 507–516, 1955.
25. **Osol, G., and M. Cipolla.** Pregnancy-induced changes in the three-dimensional mechanical properties of pressurized rat uteroplacental (radial) arteries. *Am. J. Obstet. Gynecol.* 168: 268–274, 1993.
26. **Osol, G., and W. Halpern.** Myogenic properties of cerebral blood vessels from normotensive and hypertensive rats. *Am. J. Physiol.* 249 (*Heart Circ. Physiol.* 18): H914–H921, 1985.
27. **Park, K. W., H. B. Dai, E. Lowenstein, A. Darvish, and F. W. Sellke.** Heterogeneous vasomotor responses of rabbit coronary microvessels to isoflurane. *Anesthesiology* 81: 1190–1197, 1994.
28. **Roy, C. S.** The elastic properties of the arterial wall. *J. Physiol. (Lond.)* 3: 125–159, 1880–82.
29. **Schabert, A., R. D. Bauer, and R. Busse.** Photoelectric device for the recording of diameter changes of opaque and transparent blood vessels in vitro. *Pflügers Arch.* 385: 239–242, 1980.
30. **Storkholm, J. H., O. Frøbert, and H. Gregersen.** Static elastic wall properties of the abdominal porcine aorta in vitro and in vivo. *Eur. J. Endocrinol.* 13: 31–36, 1997.
31. **Vaishnav, R. N., J. Vossoughi, D. J. Patel, L. N. Cothran, B. R. Coleman, and E. L. Ison-Franklin.** Effect of hypertension on elasticity and geometry of aortic tissue from dogs. *J. Biomech. Eng.* 112: 70–74, 1990.
32. **VanBavel, E., T. Mooij, M. J. M. M. Giezeman, and J. A. E. Spaan.** Cannulation and continuous cross-sectional area measurement of small blood vessels. *J. Pharmacol. Methods* 24: 219–227, 1990.
33. **Weber, R., N. Stergiopulos, H. R. Brunner, and D. Hayoz.** Contributions of vascular tone and structure to elastic properties of a medium-sized artery. *Hypertension* 27: 816–822, 1996.
34. **Wiederhielm, C. A.** Continuous recording of arteriolar dimension with a television microscope. *J. Appl. Physiol.* 18: 1041–1042, 1963.
35. **Wolinsky, H., and S. Glagov.** Structural basis for the static mechanical properties of the aortic media. *Circ. Res.* 14: 400–413, 1964.
36. **Wuyts, F. L., V. J. Vanhuyse, G. J. Langewouters, W. F. Decraemer, E. R. Raman, and S. Buyle.** Elastic properties of human aortas in relation to age and atherosclerosis: a structural model. *Phys. Med. Biol.* 40: 1577–1597, 1995.